JOC The Journal of Organic Chemistry

Article

pubs.acs.org/joc

Mechanistic Investigations of the $AuCl_3$-Catalyzed Nitrene Insertion into an Aromatic C—H Bond of Mesitylene

Kaipeng Hou,[†] Miao Qi,[†] Jiajun Liu,[†] Xiaoguang Bao,*[,†] and Henry F. Schaefer, III[‡]

[†]College of Chemistry, Chemical Engineering and Materials Science, Soochow University, 199 Ren-Ai Road, Suzhou Industrial Park, Suzhou, Jiangsu 215123, China

[‡]Center for Computational Quantum Chemistry, University of Georgia, Athens, Georgia 30602, United States

Supporting Information

ABSTRACT: The $AuCl_3$-catalyzed nitrene insertion into an aromatic C—H bond of mesitylene demonstrates a unique activity and chemoselectivity in direct C—H aminations. Mechanisms for catalytic nitrene insertion are examined here using theory. The $AuCl_3$ catalyst favors formation of a complex with the PhI═NNs (Ns = *p*-nitrobenzenesulfonyl) substrate, followed by the appearance of the key (*N*-chloro-4-nitrophenylsulfonamido)gold(III) chloride intermediate (**INT5**). However, the putative gold(III)-nitrene analogue ($AuCl_3$—NNs complex) is thermodynamically unfavorable compared with **INT5**. Therefore, **INT5** is suggested to play a critical role in the $AuCl_3$-promoted aromatic C—H bond amination, a prediction in contrast to the previously reported crucial metal—nitrene intermediates. The activation of a C(sp^2)—H bond of mesitylene via σ-bond metathesis is proposed based on **INT5**, and the subsequent detailed pathways for the aromatic C—H bond amination are computationally explored. A chemoselective nitrene insertion into a mesitylene aromatic C—H bond, instead of a benzylic C—H bond, is rationalized for the $AuCl_3$-catalyzed amination.

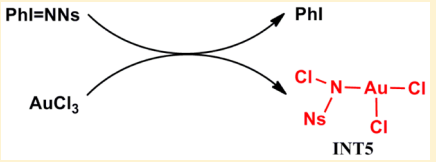

INTRODUCTION

Catalytic C—H bond amination via direct nitrene group insertion has attracted significant scientific interest.[1] This strategy promises an appealing approach to the synthesis of amines in a straightforward manner. A variety of transition-metal-based catalysts, $[M]L_n$ (M = Mn,[2,3] Fe,[2,4] Co,[5] Ni,[4b] Cu,[6] Zn,[7] Ru,[8] Rh,[9] Pd,[10] Ag,[11] and Au[12]), have been reported to promote C—H aminations using suitable nitrene precursors, such as imidoiodinanes (PhI═NR, R = Ts (*p*-toluenesulfonyl) or Ns (*p*-nitrobenzenesulfonyl)), azides, or haloamine derivatives (such as chloramines-T). In particular, producing the imidoiodinanes in situ by simply mixing an appropriate amine derivative with PhIO, $PhI(OAc)_2$, or $PhI(OPiv)_2$ offers a more synthetically convenient method in employing nitrene precursors.[1d,6g,8g,9m,n]

Except for the amination of the somewhat activated benzylic or allylic sp^3 C—H bonds, which are relatively amenable to insertion, most efforts of the past decade have been devoted to some inactivated sp^3 C—H bonds and sp^2 C—H bonds. For example, in 2013, Che and co-workers reported a highly active nonheme iron catalyst that can effectively promote amination of sp^3 C—H bonds of cyclic alkanes using PhI═NR as a nitrogen source.[4d] For sp^2 C—H bond amination, Pérez and co-workers developed a Cu—homoscorpionate complex $Tp^{Br3}Cu(NCMe)$, which shows excellent catalytic activity in inserting the nitrene group of PhI═NTs into a sp^2 C—H bond of benzene under mild conditions.[6c] Liang and Jensen reported that an Fe-based scorpionate complex can also drive the C—H amination of benzene.[4b] Moreover, He and co-workers demonstrated an $AuCl_3$-promoted nitrene insertion into an aromatic C—H bond of mesitylene, instead of a benzylic C—H bond (Scheme 1).[12] Their results represent an unusual chemoselectivity of the C—H bond amination via a direct nitrene insertion approach.

Scheme 1. $AuCl_3$-Catalyzed Nitrene Insertion into an Aromatic C—H Bond of Mesitylene Reported by He and Co-workers.[12]

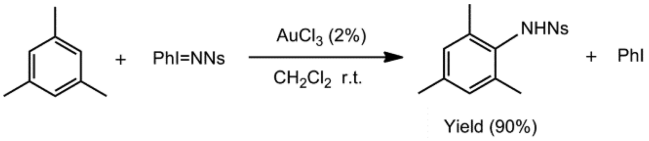

In reaction mechanisms for the transition-metal-catalyzed incorporation of a nitrene unit into C—H bonds, L_nM═N—Z intermediates have commonly been proposed to play a critical role.[1e,6f] This assumption has been supported by some isolated and structurally characterized metal—nitrene complexes.[4a,8f,13−16] For instance, Che and co-workers explored the reactions of isolated Ru—nitrene complexes, which demonstrate their activity in mediating C—H aminations.[8f] Warren and co-workers isolated a dicopper nitrene intermediate, in which a nitrene unit is bound between two β-diketiminate copper fragments.[13a] Subsequently, reactivity routes for C—H aminations via isolable nitrene-bridged dicopper complexes were examined in Warren's group.[13b] In addition, Ray and co-workers reported that a copper—nitrene intermediate was

Received: April 7, 2015
Published: May 27, 2015

DOI: 10.1021/acs.joc.5b00764
J. Org. Chem. 2015, 80, 5795−5803

Scheme 2. (a) Two Previously Proposed Mechanisms for C—H Amination Mediated by a Metal–Nitrene Intermediate and (b) a Nonmetal–Nitrene Intermediate Is Proposed in This Work

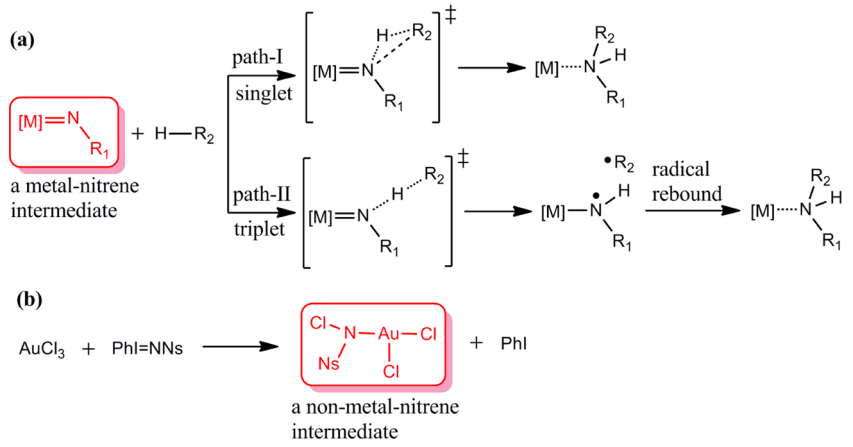

trapped with Sc(III) triflate.[14] Betley's group isolated an iron–imido compound, which is able to drive C—H bond aminations.[4a] Zhang, de Bruin, and co-workers employed electron paramagnetic resonance spectroscopy to detect a Co(III)–nitrene intermediate that accounts for C—H aminations via a stepwise radical process.[15] More recently, in 2014, bridging and terminal Cu and Ag nitrene complexes have been isolated and characterized by Bertrand and co-workers.[16]

The electronic structures of metal–nitrene intermediates have also attracted significant interest from theoretical perspectives. Copper–nitrene complexes are arguably the most extensively studied.[6f] Most of the computational studies of Cu–nitrene complexes with various auxiliary ligands suggest a triplet ground state.[6e,17] However, Cundari and co-workers performed CASSCF[18a] and ccCA[18b] computations, which indicate an open-shell singlet ground state for the (β-diketiminate)Cu(NPh) and (β-diketiminate)Cu(NH) complexes. Studies on Ni=N—Z complexes performed by Cundari's group suggested that the singlet ground states are preferred with Z = aryl/alkyl groups,[19a−c] while the triplet ground states are favored in cases where Z is an electron-withdrawing heteroatom group.[19d] A small singlet–triplet energy gap (ca. 2 kcal/mol at the CCSD(T) level of theory) was predicted for a dirhodium tetracarboxylate nitrene complex by Che's group.[9k]

On the basis of the results for metal–nitrene complexes, two plausible mechanisms have been proposed for sp^3 C—H bond aminations. One is to insert a nitrene group into the C—H bond in a concerted manner, associated with a singlet state of the metal–nitrene intermediate (path-I, Scheme 2a). The second is a stepwise mechanism that proceeds via a hydrogen atom abstraction reaction followed by a radical rebound step to yield the C—H amination product through a triplet state (path-II, Scheme 2a). Combined experimental and computational studies demonstrate that path-II is more likely for the Fe-,[4d] Ru-,[9h] Co-,[15] and Cu-mediated[13b] C—H bond aminations. On the other hand, computational studies of the dirhodium tetracarboxylate catalyzed nitrene insertion suggest that path-I is favored.[9k]

The $AuCl_3$-catalyzed nitrene insertion into an aromatic C—H bond of mesitylene under mild conditions represents an unprecedented discovery.[12] First, $AuCl_3$-promoted amination favors sp^2 C—H bonds rather than somewhat activated benzylic sp^3 C—H bonds when the mesitylene substrate is used. Second, no auxiliary ligand is needed to mediate this aromatic C—H bond amination reaction. This unique chemoselectivity and activity puts forward fascinating and potentially important mechanistic questions. Does the $AuCl_3$–nitrene intermediate, similar to the behavior of the reported[4a,8f,13−16] metal–nitrene complexes, play a critical role in driving the aromatic C—H bond amination? Otherwise, might it be possible to form a nonmetal–nitrene intermediate (shown in Scheme 2b) to account for the aromatic C—H bond amination? What are the detailed reaction pathways and the origin of this unusual chemoselectivity? In the present research, computational studies were carried out to address these questions.

RESULTS AND DISCUSSION

For the $AuCl_3$-catalyzed aromatic C—H bond amination of mesitylene with PhI=NNs, each of the two substrates may coordinate with the $AuCl_3$ catalyst to form an initial complex, mesitylene–$AuCl_3$ or PhI=NNs–$AuCl_3$. Subsequent activation pathways of mesitylene–$AuCl_3$ and PhI=NNs–$AuCl_3$ complexes to arylgold(III) and N-containing gold(III) intermediates, respectively, were computationally explored first.

Formation of the Arylgold(III) Intermediate via the Mesitylene–$AuCl_3$ Complex. He and co-workers proposed that the formation of the arylgold(III) species is the key intermediate and responsible for the selective nitrene insertion into an aromatic C—H bond.[12] Herein, the generation of the arylgold(III) intermediate from the reaction of an aromatic C—H bond of mesitylene and $AuCl_3$ was computationally explored first. The aromatic ring of mesitylene may coordinate with $AuCl_3$ to form the mesitylene–$AuCl_3$ complex (**INT1** shown in Figure 1) due to the π acidic character of gold.[20] For **INT1**, the optimized C_1···Au distance is 2.27 Å. In addition, the planar C_1 carbon of mesitylene is slightly pyramidalized due to complexation with $AuCl_3$ (the Au–C_1–H_1 angle is 94°). The formation of **INT1** is exergonic by 16.4 kcal/mol relative to separated mesitylene and $AuCl_3$. Then, the complex yielded might undergo a σ-bond metathesis reaction leading to an arylgold(III) intermediate (Figure 1). The transition state has been located for this step (**TS1**) and shows that the C_1—H_1 and Au—Cl_1 bonds are lengthened to 1.61 and 2.51 Å, respectively, whereas the C_1···Au and H_1···Cl_1 distances are shortened to 2.07 and 1.45 Å, respectively. It should be noted that, compared with **INT1**, the mesitylene moiety is in an

DOI: 10.1021/acs.joc.5b00764
J. Org. Chem. 2015, 80, 5795−5803

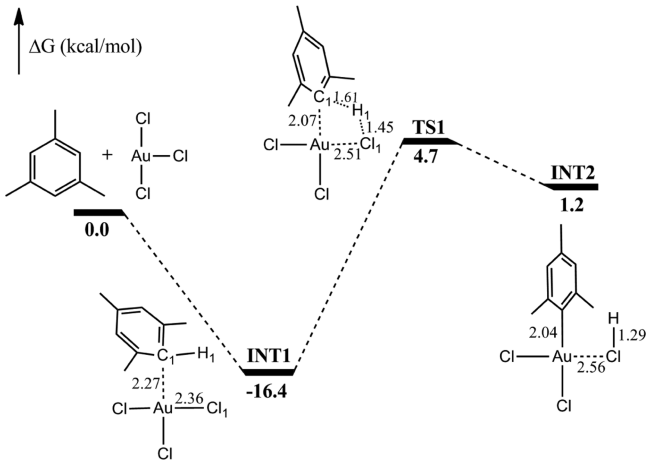

Figure 1. Free energy profile for the formation of an arylgold(III) intermediate from the mesitylene–$AuCl_3$ complex. Bond lengths are shown in Å.

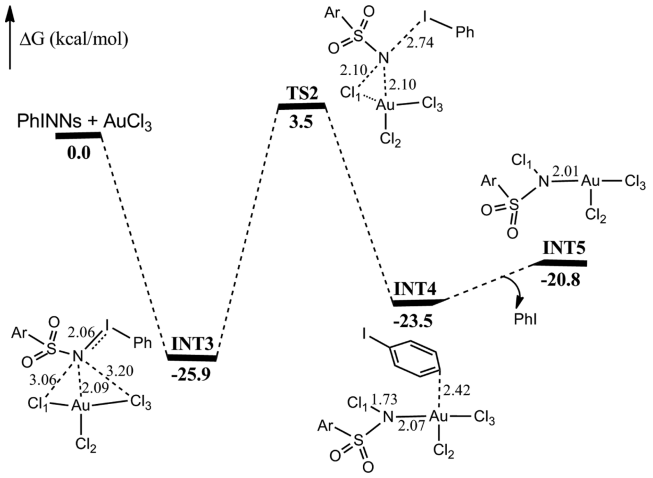

Figure 2. Free energy profile for the activation of the nitrene precursor by $AuCl_3$ to afford the intermediate **INT5**. Bond lengths are shown in Å.

almost upright position at **TS1**. The formation of the Au—C_1 bond can compensate the energy needed to break the C_1—H_1 bond. The computed activation barrier for the formation of the arylgold(III) intermediate via **TS1** is 21.1 kcal/mol. The resulting arylgold(III) intermediate coordinated with HCl (**INT2**) is very unfavorable thermodynamically, being endergonic by 17.6 kcal/mol.

The nitrene precursor, PhI=NNs, might coordinate with the yielded arylgold(III) intermediate to form **INT-S1** (see the Supporting Information, Figure S1). Subsequently, PhI=NNs might be activated by the attacking of C_1 of the aryl group to afford **INT-S2** plus PhI. The predicted energy barrier for this step is 19.5 kcal/mol. Finally, the cleavage of HCl on the Au—N bond of **INT-15** could lead to the desired product and the regeneration of the $AuCl_3$ catalyst. Computational findings suggested that the activation of a sp^2 C—H bond of mesitylene is the rate-limiting step, which is in contrast to the conclusions drawn from the experimental isotope results.[12] The inconsistency between computation and experiment might imply the existence of an alternative mechanism for the $AuCl_3$-catalyzed aromatic C—H bond amination of mesitylene with PhI=NNs.

Activation of the Nitrene Precursor by $AuCl_3$. Apart from the formation of an arylgold(III) intermediate, the activation of the nitrene precursor, PhI=NNs, promoted by $AuCl_3$ was also investigated computationally. PhI=NNs can readily coordinate with $AuCl_3$ to form an intermediate, **INT3**, in which the Au···N distance is 2.09 Å (Figure 2). Closer examination of **INT3** shows that the distance Cl_1···N (3.06 Å) is 0.14 Å shorter than that of Cl_3···N (3.20 Å). The Cl_1–Au–N angle (87.0°) deviates slightly from 90°. The existence of an in-phase combination of the lone pair AO of Cl (larger coefficient on Cl_1) and the π^* MO of the N=I moiety of PhI=NNs in the HOMO-3 orbital of **INT3** might be responsible for this structural feature (Figure 3). In addition, the insertion of the lone pair of Cl_1 into the π^* MO of the N=I moiety can result in the formation of the Cl_1—N bond and the dissociation of the PhI molecule. From **INT3**, the reaction coordinate was shown to lead to **TS2**, in which Cl_1 approaches N and the Cl_1··· N distance is shortened to 2.10 Å, while the N···I bond length is lengthened to 2.74 Å (Figure 2). Finally, PhI is dissociated from PhI=NNs, and an $AuCl_2NClNs$–PhI complex (**INT4**) is afforded.

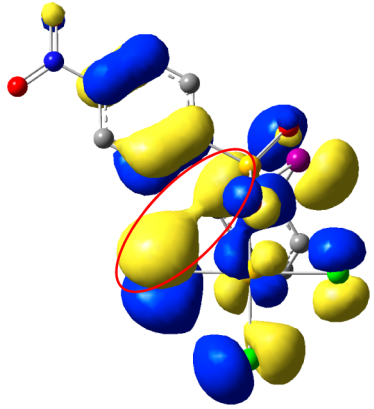

Figure 3. In-phase combination of the lone pair AO of Cl and the π^* MO of the N=I moiety of PhI=NNs in the HOMO-3 orbital of **INT3**.

The formation of **INT3** is 25.9 kcal/mol exothermic compared with separated $AuCl_3$ and PhI=NNs. The energy barrier associated with the activation of the nitrene precursor from **INT3** is predicted to be 29.4 kcal/mol. The resulted complex **INT4** is slightly endergonic, by 2.4 kcal/mol. It should be noted that the exergonicity for the formation of **INT3** is 9.5 kcal/mol larger than that for the formation of **INT1**. Therefore, it is more favorable for the $AuCl_3$ catalyst to combine with the PhI=NNs substrate than to bind with the mesitylene. Thus, the subsequent reaction of activating PhI=NNs to form **INT4** and further to yield **INT5** after a dissociation of PhI is more feasible than to form the arylgold(III) intermediate. In addition, the significant exergonicity for the formation of **INT3** can compensate the relatively higher energy needed to activate the nitrene precursor.

In the $AuCl_3$-catalyzed amination of mesitylene, the formation of the $AuCl_2NClNs$ intermediate (**INT5** in Figure 2) is unprecedented because reported transition-metal-catalyzed amination reactions by nitrene insertion usually proceed through metal–imide/nitrene complexes.[4a,8f,13−16] Just for curiosity, we computationally studied a putative gold(III)–nitrene analogue, $AuCl_3$–NNs complex, in both singlet and triplet electronic states (Figure 4). The optimized Au···N lengths are 2.09 and 2.00 Å for the singlet (**INT5a-S**) and

DOI: 10.1021/acs.joc.5b00764
J. Org. Chem. 2015, 80, 5795−5803

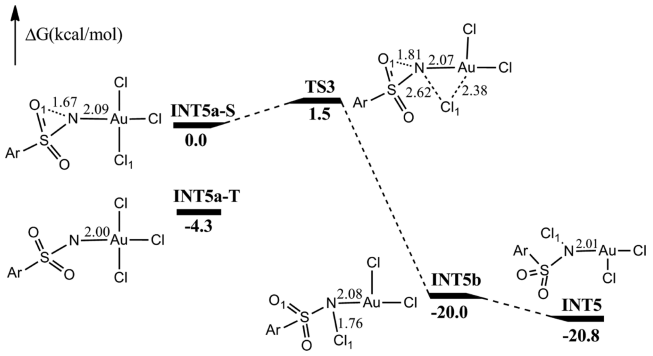

Figure 4. Optimized singlet and triplet electronic states of the gold(III)−nitrene analogue. The free energy profile for the isomerization between **INT5a-S** and **INT5** is also shown. Bond lengths are shown in Å.

triplet (**INT5a-T**) structures, respectively (Figure 4). It should be noted that the optimized singlet structure displays an unusual short $O_1\cdots N$ distance (1.67 Å). A lone pair of O_1 inserting into the empty p AO of nitrene is responsible for this short distance and the formation of a nearly three-membered ring in **INT5a-S**. The Cl_1 attached to Au(III) may attack the nitrene moiety in a manner of nucleophilic substitution to afford an intermediate **INT5b**, in which the Au—Cl_1 bond is cleaved and the N—Cl_1 bond is formed. The predicted $\Delta G^{\ddagger}$ is only 1.5 kcal/mol, indicating that **INT5a-S** is readily converted to **INT5b** via **TS3**. The structure **INT5b** may further adjust to a more energetically favorable conformation, **INT5**, which is 20.8 kcal/mol lower in energy than **INT5a-S**. For the triplet state (**INT5a-T**), inspection of the spin density of **INT5a-T** shows that the two unpaired electrons are mainly localized on the N atom (1.64), with little spin density (0.03) found on the Au atom. This is in contrast to the reported triplet Cu−nitrene complexes having significant delocalization of spin density over the metal center from the nitrene site.[17a,b] The triplet state of the $AuCl_3$−NNs complex with highly localized spin density may not be energetically favorable, a conclusion supported by the computational finding that **INT5a-T** is 16.5 kcal/mol higher in energy than **INT5** (Figure 4). Therefore, both the singlet and triplet states of the putative $AuCl_3$−NNs complex are thermodynamically unfavorable compared with **INT5**. Hence, **INT5** is suggested to be the key intermediate for the subsequent C—H bond amination.

C(sp^2)—H Bond Amination of Mesitylene Mediated by INT5. As described previously, the substrate mesitylene might coordinate with $AuCl_3$, followed by a σ-bond metathesis reaction to activate a C(sp^2)—H bond, resulting in a thermodynamically unfavorable arylgold(III) intermediate. Similarly, such a reaction route can be applied to **INT5**. There are two possible pathways to trigger a C(sp^2)—H bond activation of mesitylene in terms of the diversity of the H atom acceptor. One route is to form a complex **INT6a** and subsequently lengthen a C(sp^2)—H bond of mesitylene toward N, leading to a complex of arylgold(III) and NsNHCl (**INT7**) (pathway-a in Figure 5). The **TS4** located for pathway-a shows that the $C_1\cdots H_1$ distance is lengthened to 1.36 Å and the Au···C_1 distance is shortened to 2.10 Å, respectively. In addition, similar to **TS1**, the mesitylene moiety is also in an upright position relative to the corresponding structure of the reactant. The other route starts from **INT6b**, followed by a C(sp^2)—H bond being stretched toward Cl, which affords the formation of **INT8** (pathway-b in Figure 5). The optimized TS structure for pathway-b (**TS5**) is analogous to **TS1**.

The complex **INT6a** is 0.4 kcal/mol lower in energy than **INT6b** (Figure 5). The predicted energy barriers of pathway-a starting from **INT6a** and pathway-b from **INT6b** are 18.1 and 21.9 kcal/mol, respectively. In addition, pathway-a leading to **INT7** is slightly exergonic by 0.8 kcal/mol, whereas pathway-b affording **INT8** is quite endergonic. Therefore, pathway-a, in

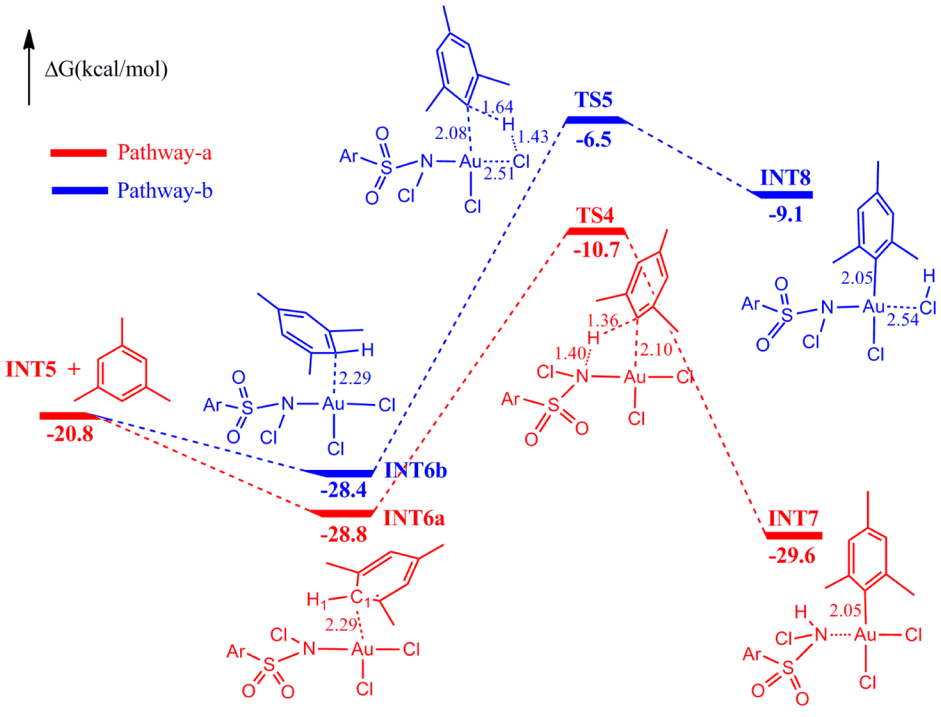

Figure 5. Free energy profiles for two pathways for activating an aromatic C—H bond of mesitylene based on **INT5**. Bond lengths are shown in Å.

DOI: 10.1021/acs.joc.5b00764
J. Org. Chem. 2015, 80, 5795−5803

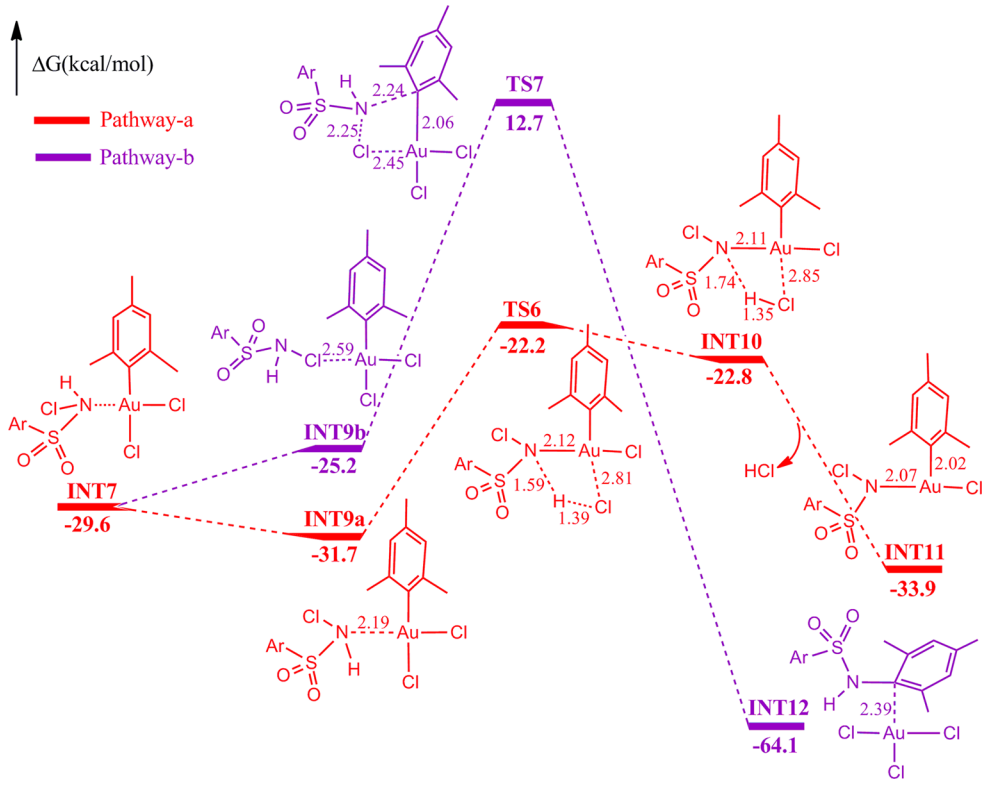

Figure 6. Free energy profiles for two possible pathways for the reaction of intermediate **INT7**. Bond lengths are shown in Å.

leading to **INT7**, is more favorable, both kinetically and thermodynamically. The N—H bond strength is greater than that of an H—Cl bond, accounting for, at least partially, the preference for pathway-a.

Apart from the above two modes of activating a C(sp^2)—H bond of mesitylene, the addition of mesitylene to the N atom of **INT5** was also explored computationally. However, the much higher energy barrier indicates that this addition pathway is unfavorable (see the Supporting Information, Figure S2).

Another two possible pathways are proposed for the subsequent reaction of the afforded **INT7** complex. One path is a σ-bond metathesis reaction to cleave the N—H bond of NsNHCl in **INT7** to eliminate an HCl and to produce an intermediate **INT10** (pathway-a in Figure 6). The other route also involves a σ-bond metathesis reaction to break the N—Cl bond of NsNHCl (pathway-b in Figure 6), yielding the desired amination product and regenerating the $AuCl_3$ catalyst (**INT12**). Pathway-a, from **INT9a** to **INT10**, has the lower energy barrier of 9.5 kcal/mol. In contrast, pathway-b, from **INT9b** to **INT12**, has a much higher energy barrier (37.9 kcal/mol). Thus, the pathway-a leading to **INT10** is more likely to occur.

The dissociation of HCl following the formation of complex **INT10** can result in **INT11**. Next, structure **INT11** may undergo a reductive elimination reaction to produce an Au(I) intermediate (**INT13**). The reductive elimination of **INT11** proceeds via a three-membered ring transition state, where the N—C_1 bond (2.04 Å) is being formed and the Au—C_1 bond is breaking (2.24 Å) (**TS8** in Figure 7). The reductive elimination via **TS8** requires an activation barrier of 29.2 kcal/mol. The resulting **INT13** lies 3.9 kcal/mol below **INT11**. In **INT13**, the AuCl intermediate is coordinated with a N atom. Switching the binding site of the Au center from N to Cl can result in a more favorable intermediate **INT14**, 12.6 kcal/mol below **INT13**. The conversion from **INT14** to **INT15** can lead to an intermediate lower in energy by ΔG = 13.1 kcal/mol. With the participation of HCl, an intermediate **INT16** is formed. It is facile for HCl to transfer a proton to the N atom of **INT16**, with $\Delta G^{\ddagger}$ = 2.7 kcal/mol. This leads to the desired product and regenerates the initial $AuCl_3$ catalyst.

Our computational studies find that the step of activation of the nitrene precursor by the $AuCl_3$ catalyst to form **INT5** and the reductive elimination step from **INT11** to form **INT13** have almost the same energy barrier (ca. 29 kcal/mol) and thus contribute almost equally to the rate-limiting step for the $AuCl_3$-catalyzed nitrene insertion into an aromatic C—H bond of mesitylene. Nevertheless, the aromatic C—H bond activation via a σ-bond metathesis mechanism is not suggested to be the rate-limiting step due to the relatively lower energy barrier. Therefore, kinetic isotope effects of H/D for the mesitylene substrate should not be significant, consistent with the experimental results.[12] The substantial exothermicity of the amination reaction could assist to overcome the relatively higher energy barrier at room temperature.

C(sp^3)—H Bond Amination of Mesitylene Mediated by INT5. According to the research described above, the N site of **INT5** is more favorable than the Cl site as an H atom acceptor for activating a C(sp^2)—H bond of mesitylene via the σ-bond metathesis pathway. Thus, activation of a C(sp^3)—H bond of mesitylene is focused on the N site of **INT5**. From the energetically favorable complex **INT6a**, except for the previously studied C(sp^2)—H bond cleavage of mesitylene, a benzylic C(sp^3)—H bond activation was also investigated (pathway-a in Figure 8). The transition state for the H atom transfer reaction (**TS10**) is shown in Figure 8, in which the $C_1 \cdots H_1$ distance is lengthened to 1.47 Å and the $N \cdots H_1$ distance is shortened to 1.21 Å. The predicted $\Delta G^{\ddagger}$ for the cleavage of the benzylic C(sp^3)—H bond is 25.7 kcal/mol,

DOI: 10.1021/acs.joc.5b00764
J. Org. Chem. 2015, 80, 5795−5803

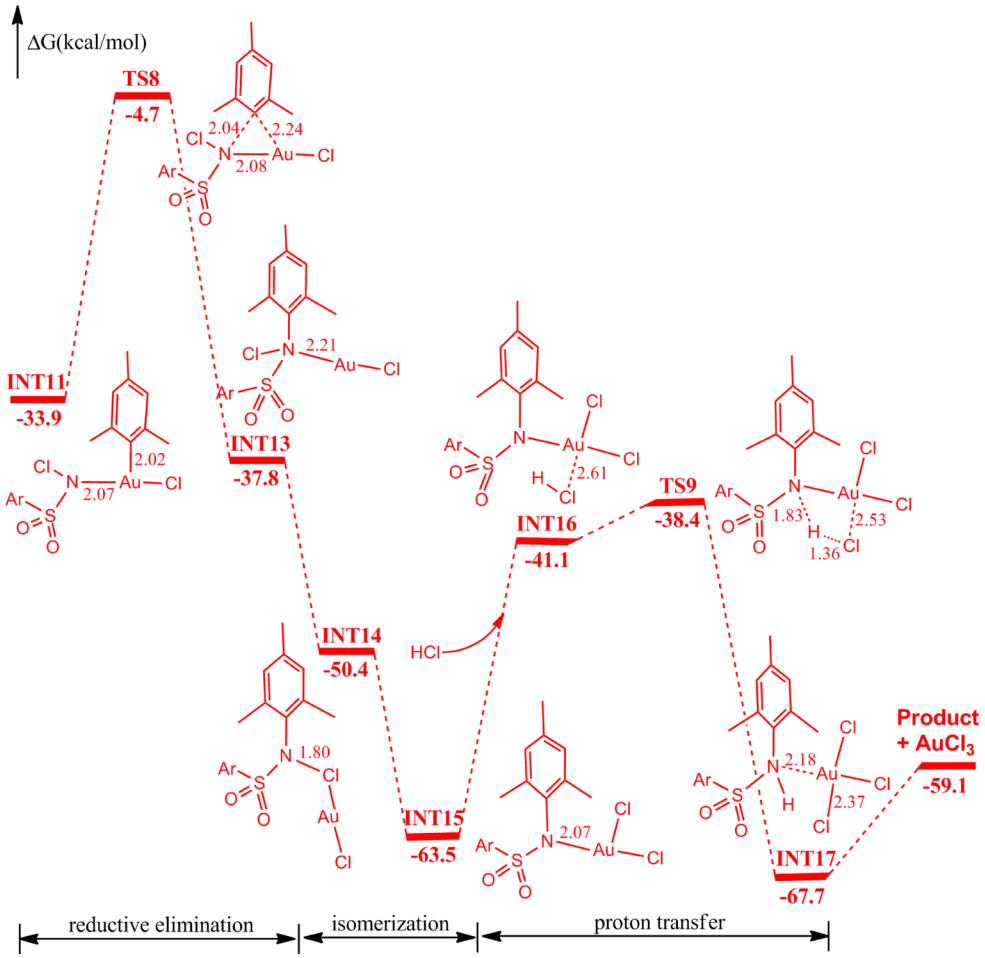

Figure 7. Free energy profile for the further conversion of **INT13** to the final product. Bond lengths are shown in Å.

which is 7.6 kcal/mol higher than that for the breaking of a C(sp^2)—H bond of mesitylene.

The second activation route of a C(sp^3)—H bond of mesitylene involves a direct σ-bond metathesis pathway (pathway-b in Figure 8). The geometry of the transition state (**TS11**) illustrates that the $C_1\cdots H_1$ and Au···N distances are lengthened to 1.34 and 2.12 Å, respectively, whereas the distances Au···C_1 and N···H_1 are shortened to 2.36 and 1.43 Å, respectively. The relative energy of **TS11** is 4.9 kcal/mol higher than that of **TS10**. In addition, pathway-b does not start from a thermodynamically favorable reactant complex (**INT6c**). Therefore, pathway-b is even more unfavorable. The present computational studies suggest that the cleavage of a C(sp^3)—H bond of mesitylene is less likely to occur compared with the breaking of a C(sp^2)—H bond, in good agreement with experimental observations.[12]

Why does a C(sp^3)—H bond of mesitylene, which has a smaller bond dissociation energy (BDE) compared with that for a C(sp^2)—H bond, have a higher energy barrier for amination? It should be noted that the complex **INT6a** is ready to be formed prior to the favorable reaction pathway leading to either C(sp^2)—H bond breaking or C(sp^3)—H bond breaking. Closer examination of pathway-a in Figure 5 reveals that the breaking of an aromatic C—H bond does not destroy the aromaticity of mesitylene. In addition, the Au—C_1(sp^2) bond formed in **TS4** (2.10 Å) can compensate effectively for the energy needed to break an aromatic C—H bond. In contrast, the cleavage of a benzylic C—H bond destroys the aromaticity of mesitylene (pathway-a in Figure 8). The resulting much longer Au—C_2(sp^3) bond distance in **TS10** (2.32 Å) compared with the corresponding Au—C_1(sp^2) bond in **TS4** implies a lower effectiveness in stabilizing **TS10**. Thus, a thermodynamically very unfavorable intermediate (**INT18**) is afforded. Therefore, although the strength of a benzylic C—H bond of mesitylene is weaker than that of an aromatic C—H bond, the cleavage of a benzylic C—H bond results in damage of the aromaticity of mesitylene. Consequently, the extra energy penalty imposed by the breaking of the aromaticity leads to an overall much higher activation energy barrier for the cleavage of a benzylic C—H bond. Hence, the breaking of an aromatic C—H bond of mesitylene is much more favorable, and the product of the chemoselective nitrene insertion into an aromatic C—H bond is attained.[12]

■ CONCLUSIONS

In the present research, the $AuCl_3$-catalyzed nitrene insertion into an aromatic C—H bond of mesitylene has been explored mechanistically. In summary, it is more favorable for the $AuCl_3$ catalyst to combine with the PhI═NNs substrate than to bind with the mesitylene. Thus, the subsequent activation reaction of PhI═NNs to form **INT5** is more likely to occur. The putative $AuCl_3$–NNs complex is computed to be energetically unfavorable and may not play a critical role in the $AuCl_3$-promoted C(sp^2)—H bond amination, in contrast to previously reported key metal–imide/nitrene intermediates.

DOI: 10.1021/acs.joc.5b00764
J. Org. Chem. 2015, 80, 5795−5803

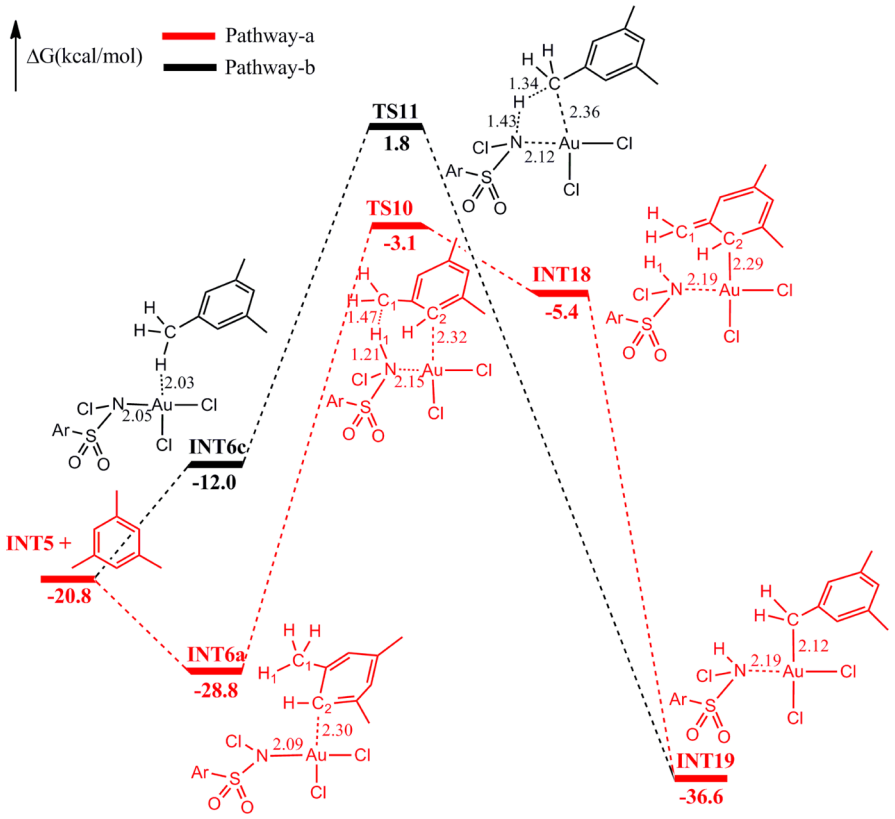

Figure 8. Free energy profiles for two pathways for the activation of a benzylic C—H bond of mesitylene. Bond lengths are shown in Å.

Instead, **INT5** is proposed to play a vital role in the subsequent amination reaction.

A detailed C(sp^2)—H bond amination pathway of mesitylene is proposed in the present computational research (Scheme 3). After the complexation of **INT5** with mesitylene, activation of a C(sp^2)—H bond in a manner of σ-bond metathesis leading to **INT7** is favored. From **INT7**, another σ-bond metathesis reaction to eliminate an HCl and produce **INT11** can occur. Then, the resulting **INT11** may undergo a reductive elimination reaction to afford **INT13**, which may proceed to the lower energy intermediate **INT15**. Finally, with the participation of HCl, a proton transfer step follows to yield the desired amination product and to regenerate the $AuCl_3$ catalyst.

Scheme 3. Proposed Mechanism for the $AuCl_3$-Catalyzed Nitrene Insertion into an Aromatic C—H Bond of Mesitylene

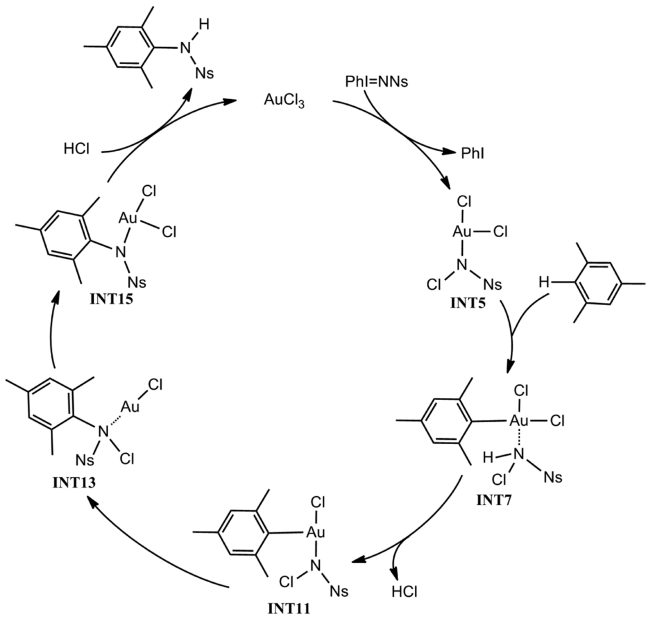

Chemoselective nitrene insertion into an aromatic C—H bond of mesitylene, instead of a benzylic C—H bond, is also rationalized for the $AuCl_3$-promoted amination. In spite of the smaller BDE of a benzylic C—H bond of mesitylene in comparison with that of an aromatic C—H bond, the cleavage of a benzylic C—H bond leads to damage of the aromaticity of the mesitylene moiety, which results in an overall higher energy barrier. In contrast, the aromaticity of mesitylene is retained for the aromatic C—H bond activation. Consequently, the aromatic C—H bond amination is more favorable, in good agreement with experimental results. These mechanistic insights reported herein should encourage further development of chemoselective C—H bond functionalizations.

COMPUTATIONAL METHODS

The PBE0[21] density functional method, which has shown good performance in gold-catalyzed reactions,[22] was employed in this work to carry out all the computations. The LANL2DZ basis set in conjunction with the LANL2DZ pseudopotential[23] was used for the Au atom, and the LANL2DZdp basis set with the LANL2DZ pseudopotential[23] was used for the I atom. The 6-31G(d) basis set[24] was used for the other atoms in the geometry optimizations. Vibrational frequency analyses at the same level of theory were performed on all optimized structures to characterize stationary points as local minima or transition states. Transition states were verified to

DOI: 10.1021/acs.joc.5b00764
J. Org. Chem. 2015, 80, 5795−5803

have one imaginary vibrational frequency and were connected to appropriate reactant and product by optimizations along the reaction coordinate. The gas-phase Gibbs free energies for all species were obtained at 298.15 K and 1 atm at their respective optimized structures.

To consider solvation effects, single-point energy computations using the polarizable continuum model model[25] with dichloromethane as the solvent were performed based on the optimized gas-phase geometries of all species. Larger basis sets (LANL2TZ(f) for Au, LANL2DZdp for I, and 6-311++G(2d,2p) for other atoms) were utilized for single-point energy calculations on stationary points. The solution-phase Gibbs free energy was determined by adding the solvation single-point energy and the gas-phase thermal correction to the Gibbs free energy obtained from the vibrational frequencies. Unless otherwise specified, the solution-phase Gibbs free energy was used in the present discussions. The Gaussian 09 suite of programs[26] was used throughout.

■ ASSOCIATED CONTENT

Supporting Information

Free energy profile for the activation of PhI=NNs by the arylgold(III) intermediate and subsequent conversion to the final product; free energy profile for the addition of mesitylene to the N atom of **INT5** and subsequent transformation to the final product; optimized geometries and energies; and a complete ref 26. The Supporting Information is available free of charge on the ACS Publications website at DOI: 10.1021/acs.joc.5b00764.

■ AUTHOR INFORMATION

Corresponding Author

*E-mail: xgbao@suda.edu.cn.

Notes

The authors declare no competing financial interest.

■ ACKNOWLEDGMENTS

X.B. is supported by the Natural Science Foundation of China (NSFC 21302133), the startup fund from the Soochow University, and the Priority Academic Program Development of Jiangsu Higher Education Institutions (PAPD). H.F.S. is supported by the U.S. National Science Foundation, grant CHE-1361178.

■ REFERENCES

(1) (a) Müller, P.; Fruit, C. *Chem. Rev.* **2003**, *103*, 2905. (b) Chang, J. W. W.; Ton, T. M. U.; Chan, P. W. H. *Chem. Rec.* **2011**, *11*, 331. (c) Cenini, S.; Gallo, E.; Caselli, A.; Ragaini, F.; Fantauzzi, S.; Piangiolino, C. *Coord. Chem. Rev.* **2006**, *250*, 1234. (d) Roizen, J. L.; Harvey, M. E.; Du Bois, J. *Acc. Chem. Res.* **2012**, *45*, 911. (e) Díaz-Requejo, M. M.; Pérez, P. J. *Chem. Rev.* **2008**, *108*, 3379.

(2) Breslow, R.; Gellman, S. H. *J. Am. Chem. Soc.* **1983**, *105*, 6728.

(3) Zhang, J.; Chan, P. W. H.; Che, C.-M. *Tetrahedron Lett.* **2005**, *46*, 5403.

(4) (a) King, E. R.; Hennessy, E. T.; Betley, T. A. *J. Am. Chem. Soc.* **2011**, *133*, 4917. (b) Liang, S.; Jensen, M. P. *Organometallics* **2012**, *31*, 8055. (c) Hennessy, E. T.; Betley, T. A. *Science* **2013**, *340*, 591. (d) Liu, Y.; Guan, X.; Wong, E. L.-M.; Liu, P.; Huang, J.-S.; Che, C.-M. *J. Am. Chem. Soc.* **2013**, *135*, 7194. (e) Hennessy, E. T.; Liu, R. Y.; Iovan, D. A.; Duncan, R. A.; Betley, T. A. *Chem. Sci.* **2014**, *5*, 1526.

(5) King, E. R.; Sazama, G. T.; Betley, T. A. *J. Am. Chem. Soc.* **2012**, *134*, 17858.

(6) (a) Albone, D. P.; Aujla, P. S.; Taylor, P. C.; Challenger, S.; Derrick, A. M. *J. Org. Chem.* **1998**, *63*, 9569. (b) Hamilton, C. W.; Laitar, D. S.; Sadighi, J. P. *Chem. Commun.* **2004**, 1628. (c) Díaz-Requejo, M. M.; Belderraín, T. R.; Nicasio, M. C.; Trofimenko, S.; Pérez, P. J. *J. Am. Chem. Soc.* **2003**, *125*, 12078. (d) Fructos, M. R.; Trofimenko, S.; Díaz-Requejo, M. M.; Pérez, P. J. *J. Am. Chem. Soc.* **2006**, *128*, 11784. (e) Barman, D. N.; Liu, P.; Houk, K. N.; Nicholas, K. M. *Organometallics* **2010**, *29*, 3404. (f) Gephart, R. T.; Warren, T. H. *Organometallics* **2012**, *31*, 7728. (g) Dauban, P.; Sanière, L.; Tarrade, A.; Dodd, R. H. *J. Am. Chem. Soc.* **2001**, *123*, 7707. (h) Bagchi, V.; Paraskevopoulou, P.; Das, P.; Chi, L.; Wang, Q.; Choudhury, A.; Mathieson, J. S.; Cronin, L.; Pardue, D. B.; Cundari, T. R.; Motrikas, G.; Sanakis, Y.; Stavropoulos, P. *J. Am. Chem. Soc.* **2014**, *136*, 11362.

(7) Kalita, B.; Lamar, A. A.; Nicholas, K. M. *Chem. Commun.* **2008**, 4291.

(8) (a) Au, S.-M.; Huang, J.-S.; Che, C.-M.; Yu, W.-Y. *J. Org. Chem.* **2000**, *65*, 7858. (b) Liang, J.-L.; Yu, X.-Q.; Che, C.-M. *Chem. Commun.* **2002**, 124. (c) Liang, J.-L.; Yuan, S.-X.; Huang, J.-S.; Che, C.-M. *J. Org. Chem.* **2004**, *69*, 3610. (d) Au, S.-M.; Zhang, S.-B.; Fung, W.-H.; Yu, W.-Y.; Che, C.-M.; Cheung, K.-K. *Chem. Commun.* **1998**, 2677. (e) He, L.; Chan, P. W. H.; Tsui, W.-M.; Yu, W.-Y.; Che, C.-M. *Org. Lett.* **2004**, *6*, 2405. (f) Au, S.-M.; Huang, J.-S.; Yu, W.-Y.; Fung, W.-H.; Che, C.-M. *J. Am. Chem. Soc.* **1999**, *121*, 9120. (g) Yu, X.-Q.; Huang, J.-S.; Zhou, X.-G.; Che, C.-M. *Org. Lett.* **2000**, *2*, 2233.

(9) (a) Liang, J.-L.; Yuan, S.-X.; Chan, P. W. H.; Che, C.-M. *Org. Lett.* **2002**, *4*, 4507. (b) Lebel, H.; Huard, K.; Lectard, S. *J. Am. Chem. Soc.* **2005**, *127*, 14198. (c) Liang, C.; Robert-Peillard, F.; Fruit, C.; Müller, P.; Dodd, R. H.; Dauban, P. *Angew. Chem., Int. Ed.* **2006**, *45*, 4641. (d) Reddy, R. P.; Davies, H. M. L. *Org. Lett.* **2006**, *8*, 5013. (e) Fiori, K. W.; Du Bois, J. *J. Am. Chem. Soc.* **2007**, *129*, 562. (f) Liang, C.; Collet, F.; Robert-Peillard, F.; Müller, P.; Dodd, R. H.; Dauban, P. *J. Am. Chem. Soc.* **2008**, *130*, 343. (g) Zalatan, D. N.; Du Bois, J. *J. Am. Chem. Soc.* **2008**, *130*, 9220. (h) Harvey, M. E.; Musaev, D. G.; Du Bois, J. *J. Am. Chem. Soc.* **2011**, *133*, 17207. (i) Bess, E. N.; DeLuca, R. J.; Tindall, D. J.; Oderinde, M. S.; Roizen, J. L.; Du Bois, J.; Sigman, M. S. *J. Am. Chem. Soc.* **2014**, *136*, 5783. (j) Zhang, X.; Ke, Z.; DeYonker, N. J.; Xu, H.; Li, Z.-F.; Xu, X.; Zhang, X.; Su, C.-Y.; Phillips, D. L.; Zhao, C. *J. Org. Chem.* **2013**, *78*, 12460. (k) Lin, X.; Zhao, C.; Che, C.-M.; Ke, Z.; Phillips, D. L. *Chem.—Asian J.* **2007**, *2*, 1101. (l) Zhang, X.; Xu, H.; Zhao, C. *J. Org. Chem.* **2014**, *79*, 9799. (m) Padwa, A.; Stengel, T. *Org. Lett.* **2002**, *4*, 2137. (n) Espino, C. G.; Du Bois, J. *Angew. Chem., Int. Ed.* **2001**, *40*, 598.

(10) (a) Beccalli, E. M.; Broggini, G.; Martinelli, M.; Sottocornola, S. *Chem. Rev.* **2007**, *107*, 5318. (b) Dick, A. R.; Remy, M. S.; Kampf, J. W.; Sanford, M. S. *Organometallics* **2007**, *26*, 1365. (c) Brice, J. L.; Harang, J. E.; Timokhin, V. I.; Anastasi, N. R.; Stahl, S. S. *J. Am. Chem. Soc.* **2005**, *127*, 2868. (d) Ke, Z.; Cundari, T. R. *Organometallics* **2010**, *29*, 821.

(11) (a) Cui, Y.; He, C. *Angew. Chem., Int. Ed.* **2004**, *43*, 4210. (b) Gómez-Emeterio, B. P.; Urbano, J.; Díaz-Requejo, M. M.; Pérez, P. J. *Organometallics* **2008**, *27*, 4126.

(12) Li, Z.; Capretto, D. A.; Rahaman, R. O.; He, C. *J. Am. Chem. Soc.* **2007**, *129*, 12058.

(13) (a) Badiei, Y. M.; Dinescu, A.; Dai, X.; Palomino, R. M.; Heinemann, F. W.; Cundari, T. R.; Warren, T. H. *Angew. Chem., Int. Ed.* **2008**, *47*, 9961. (b) Aguila, M. J. B.; Badiei, Y. M.; Warren, T. H. *J. Am. Chem. Soc.* **2013**, *135*, 9399.

(14) Kundu, S.; Miceli, E.; Farquhar, E.; Pfaff, F. F.; Kuhlmann, U.; Hildebrandt, P.; Ray, K. *J. Am. Chem. Soc.* **2012**, *134*, 14710.

(15) Lyaskovskyy, V.; Suarez, A. I. O.; Lu, H.; Jiang, H.; Zhang, X. P.; de Bruin, B. *J. Am. Chem. Soc.* **2011**, *133*, 12264.

(16) Dielmann, F.; Andrada, D. M.; Frenking, G.; Bertrand, G. *J. Am. Chem. Soc.* **2014**, *136*, 3800.

(17) (a) Maestre, L.; Sameera, W. M. C.; Díaz-Requejo, M. M.; Maseras, F.; Pérez, P. J. *J. Am. Chem. Soc.* **2013**, *135*, 1338. (b) Brandt, P.; Södergren, M. J.; Andersson, P. G.; Norrby, P.-O. *J. Am. Chem. Soc.* **2000**, *122*, 8013. (c) Conradie, J.; Ghosh, A. *J. Chem. Theory Comput.* **2007**, *3*, 689.

(18) (a) Cundari, T. R.; Dinescu, A.; Kazi, A. B. *Inorg. Chem.* **2008**, *47*, 10067. (b) Tekarli, S. M.; Williams, T. G.; Cundari, T. R. *J. Chem. Theory Comput.* **2009**, *5*, 2959.

(19) (a) Cundari, T. R.; Vaddadi, S. *J. Mol. Struct.* **2006**, *801*, 47. (b) Cundari, T. R.; Pierpont, A. W.; Vaddadi, S. *J. Organomet. Chem.*

DOI: 10.1021/acs.joc.5b00764
J. Org. Chem. 2015, 80, 5795−5803

2007, *692*, 4551. (c) Cundari, T. R.; Jiminez-Halla, J. O. C.; Morello, G. R.; Vaddadi, S. *J. Am. Chem. Soc.* **2008**, *130*, 13051. (d) Cundari, T. R.; Morello, G. R. *J. Org. Chem.* **2009**, *74*, 5711.
(20) For a review, see Fürstner, A.; Davies, P. W. *Angew. Chem., Int. Ed.* **2007**, *46*, 3410.
(21) (a) Perdew, J. P.; Burke, K.; Ernzerhof, M. *Phys. Rev. Lett.* **1996**, *77*, 3865. (b) Ernzerhof, M.; Scuseria, G. E. *J. Chem. Phys.* **1999**, *110*, 5029. (c) Adamo, C.; Barone, V. *J. Chem. Phys.* **1999**, *110*, 6158.
(22) Kang, R.; Chen, H.; Shaik, S.; Yao, J. *J. Chem. Theory Comput.* **2011**, *7*, 4002.
(23) Hay, P. J.; Wadt, W. R. *J. Chem. Phys.* **1985**, *82*, 299.
(24) Hehre, W. J.; Ditchfield, R.; Pople, J. A. *J. Chem. Phys.* **1972**, *56*, 2257.
(25) (a) Miertus, S.; Scrocco, E.; Tomasi, J. *Chem. Phys.* **1981**, *55*, 117. (b) Tomasi, J.; Mennucci, B.; Cammi, R. *Chem. Rev.* **2005**, *105*, 2999.
(26) Frisch, M. J.; Trucks, G. W.; Schlegel, H. B.; Scuseria, G. E.; Robb, M. A.; Cheeseman, J. R.; Scalmani, G.; Barone, V.; Mennucci, B.; Petersson, G. A.; et al. *Gaussian 09*, Revision C.01; Gaussian, Inc.: Wallingford, CT, 2010.

DOI: 10.1021/acs.joc.5b00764
J. Org. Chem. 2015, 80, 5795−5803